

Coenzyme B₁₂ Axial-Base Chemical Precedent Studies.[†] Adenosylcobinamide Plus Sterically Hindered Axial-Base Co–C Bond Cleavage Product and Kinetic Studies: Evidence for the Dominance of Axial-Base Transition-State Effects and for Co–N(Axial-Base) Distance-Dependent, Competing σ and π Effects

Jeanne M. Sirovatka and Richard G. Finke*

Department of Chemistry, Colorado State University, Fort Collins, Colorado 80523

Received June 1, 1998

Adenosylcobinamide (AdoCbi⁺) plus the sterically hindered bases 1,2-dimethylimidazole, 2-methylpyridine, and 2,6-dimethylpyridine, as well as control experiments with imidazolate and 4-methylimidazolate, have been investigated to provide chemical precedent for the benzimidazole base-off, protein histidine imidazole base-on form of adenosylcobalamin (AdoCbl, also coenzyme B₁₂). This imidazole base-on form of AdoCbl was observed in the recent X-ray crystallographic structural study of methylmalonyl-CoA (MMCoA) mutase; of interest to the present work is the fact that MMCoA mutase contains a long, ca. 2.5 Å, Co–N(imidazole) axial bond, at least in the enzyme's crystallographically characterized Co^{II}/Co^{III} state and conformation. In the present studies, upper limits for the axial-base binding K_{assoc} parameters to form [AdoCbi·bulky base]⁺ BF₄[−] have been obtained; these thermodynamic studies reveal that sterically hindered bases do *not* bind detectably to AdoCbi⁺ in the ground state, which results in negligible ground-state free-energy stabilization via the formation of [AdoCbi·bulky base]⁺. The sterically hindered bases do, however, bind to Co^{II}Cbi⁺, a good energetic model of the [Ado· · · · CoCbi]⁺ homolysis transition state. Kinetic studies demonstrate that the sterically hindered bases *are* involved in the rate-determining step of Co–C bond homolysis, accelerating it by 200-fold; hence, Co–C cleavage does occur via the low-level and otherwise nondetectable amount of [AdoCbi·bulky base]⁺ formed in solution. Product studies reveal (i) that both Co–C heterolysis and homolysis occur, and (ii) that there is no simple correlation between the ratio of Co–C heterolysis to homolysis and the Co–N(axial-base) bond length. Overall, the results provide strong evidence for the dominance of axial-base transition-state effects on Co–C bond cleavage, and reveal a subtle interplay of σ and π effects as a function of the Co–N(axial-base) bond length.

Introduction

The recent X-ray crystallographic investigation of coenzyme B₁₂ (adocobalamin, AdoCbl¹)-dependent methylmalonyl-CoA (MMCoA) mutase^{2a} revealed that a protein side-chain histidine imidazole, rather than B₁₂'s intramolecularly appended 5,6-dimethylbenzimidazole, serves as the axial base coordinated with cobalt.³ The Co–N(imidazole) bond length is unusually long, ca. 2.5 Å in the mixed Co^{II}/Co^{III} state and conformation of MMCoA mutase characterized crystallographically.^{2a} An ex-

tended X-ray absorption fine structure (EXAFS) study revealed a similar Co–N bond length of 2.45 ± 0.05 Å in one of two fits to the EXAFS data.^{2b} Hence, the question arises: What is the purpose of the 5,6-dimethylbenzimidazole base-off, but imidazole base-on, motif in MMCoA mutase vs the appended 5,6-dimethylbenzimidazole base-on motif that occurs in the other subclass B₁₂-dependent enzymes such as diol dehydratase or ribonucleotide reductase?

Recent axial-base chemical precedent studies for imidazole coordination and Co–C cleavage^{4b,5} in the adenosylcobinamide-*N*-methylimidazole complex ([AdoCbi·*N*-MeIm]⁺, Figure 1, base = *N*-methylimidazole) revealed the unexpected result that *N*-MeIm accelerates *both* Co–C homolysis and heterolysis by a record 870- and 30 700-fold vs the reference point of [AdoCbi·solvent]⁺ (solvent = ethylene glycol).^{5a} A detailed examination of the *N*-MeIm vs pyridine and Me₂N-pyridine homolysis and heterolysis data revealed that strong σ donors favor Co–C heterolysis; those studies^{5a} also revealed that the Co–C *homolysis* data *cannot* be explained by σ effects alone and led to the postulate that π effects must be involved in achieving *N*-MeIm's acceleration of Co–C homolytic cleavage.

The following prediction emerges for imidazole axial bases *with varying Co–N bond distances* if one combines our previous

[†] Part 4 of a series.^{4a,b,5a}

- (1) Abbreviations used: AdoCbl, coenzyme B₁₂, adocobalamin, 5'-deoxy-5'-adenosylcobalamin; AdoCbi⁺, AdoCbi⁺ BF₄[−], adocobinamide, 5'-deoxy-5'-adenosylcobinamide; Co^{II}Cbi⁺ cob^{II}inamide; MMCoA mutase, methylmalonyl-CoA mutase; TEMPO, 2,2,6,6-tetramethylpiperidinyl-1-oxy; py, pyridine; *N*-ImH, imidazole; 2-Mepy, 2-methylpyridine, 2-picoline; 2,6-Me₂py, 2,6-dimethylpyridine, 2,6-lutidine; *N*-MeIm, *N*-methylimidazole, Im[−], imidazolate anion; bzm, benzimidazole.
- (2) (a) Mancia, F.; Keep, N. H.; Nakagawa, A.; Leadlay, P. F.; McSweeney, S.; Rasmussen, B.; Bösecke, P.; Diat, O.; Evans, P. R. *Structure* **1996**, *4*, 339. (b) Scheuring, E.; Padmakumar, R.; Banerjee, R.; Chance, M. R. *J. Am. Chem. Soc.* **1997**, *119*, 12192. It should be noted that two mathematically acceptable solutions are reported as a result of the global mapping technique used to analyze the EXAFS data, one corresponding to a long Co–N bond length, 2.45 ± 0.05 Å, and one corresponding to a more normal Co–N bond length, 2.13 ± 0.04 Å.
- (3) This motif was first discovered for MeB₁₂ bound to methionine synthase: Drennan, C. L.; Huang, S.; Drummond, J. T.; Matthews, R. G.; Ludwig, M. L. *Science* **1994**, *266*, 1669.

- (4) (a) Part 1. Garr, C. D.; Sirovatka, J. M.; Finke, R. G. *Inorg. Chem.* **1996**, *35*, 5912. (b) Part 2. Garr, C. D.; Sirovatka, J. M.; Finke, R. G. *J. Am. Chem. Soc.* **1996**, *118*, 11142.

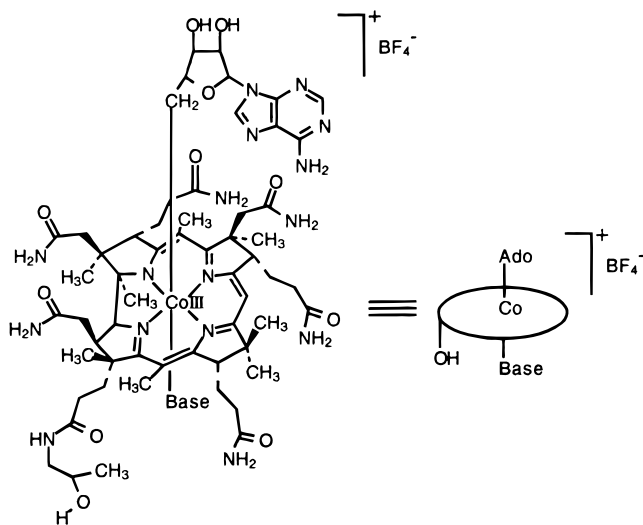


Figure 1. The molecular structure and schematic representation of 5'-deoxy-5'-adenosylcobinamide ($\text{AdoCbi}^+\text{base}^+ \text{BF}_4^-$), where base is either solvent (ethylene glycol) or an added, exogenous base.

chemical precedent studies^{5a} with molecular orbital calculations on a model complex (Me-Co-NH_2) which examines $-\text{NH}_2$ σ effects alone:⁶ at very long Co-N (imidazole) bond lengths (i.e., where π effects are completely attenuated), σ effects alone will dominate the Co-C bond cleavage but will be weak, and homolysis alone should occur. At shorter Co-N (imidazole) bond lengths, both σ and π effects^{5a} will influence the reaction, and a combination of homolysis and heterolysis should occur, with heterolysis dominating for the shortest Co-N bonds and the strongest σ -donor axial bases. This prediction is one that has not been tested experimentally until now.

Herein we report the results of adocobinamide•bulky base ($[\text{AdoCbi}\cdot\text{bulky base}]^+$) Co-C thermolytic cleavage product studies, kinetic studies, and axial-base binding studies (K_{assoc} or limits to K_{assoc}), for the *sterically encumbered axial bases* 1,2-dimethylimidazole (1,2- Me_2Im), 2-methylpyridine (2-Mepy or 2-picoline), and 2,6-dimethylpyridine (2,6- Me_2py or 2,6-

lutidine). Also reported as control studies are $[\text{AdoCbi}\cdot\text{base}]^+$ studies using the simple bases imidazole (N-Im) and imidazolone (Im^-). The results reveal (i) that sterically encumbered bases with long Co-N (axial-base) distances show *no detectable ground-state* coordination to AdoCbi^+ , (ii) that sterically encumbered bases do, however, bind to $\text{Co}^{\text{II}}\text{Cbi}^+$, implying that coordination of the base to the $\text{Co}^{\text{II}}\text{Cbi}^+$ -like transition state for Co-C homolysis is possible, (iii) that the sterically encumbered bases *are* involved in the rate-determining step of Co-C bond cleavage as demonstrated by the first-order dependence of the kinetics upon added sterically hindered base, and (iv) that, therefore, sterically encumbered axial bases exhibit their effects primarily at the transition state for Co-C bond homolysis. Our results also show (v) that there is no simple correlation between the length of the Co-N bond and the mode of Co-C bond cleavage, a perhaps not unexpected result given the different dependencies of σ vs π effects upon the Co-N (axial-base) distance.

Results

Selection of Sterically Hindered Axial Bases. Appropriate nitrogenous axial bases (that would generate long Co-N bond lengths) were selected from the bases used by Marzilli, Randaccio, and their co-workers⁷ in their X-ray crystal structures of the B_{12} model complexes cobaloximes; specifically, a 0.028(4) Å increase in the Co-N bond length is seen when comparing the crystal structures of the cobaloxime ($\text{Co}(\text{DH})_2$) complexes $[\text{MeCo}(\text{DH})_2]_1,2\text{-Me}_2\text{Im}$ and $[\text{MeCo}(\text{DH})_2]_2\text{-N-MeIm}$ (the former having the more sterically hindered base, 1,2- Me_2Im , vs simple N-MeIm).^{7b} Similarly, an increase of 0.095(3) Å in the Co-N bond length is seen in the crystal structures of $[(\text{CH}(\text{CH}_3)_2\text{Co}(\text{DH})_2\text{-NH}_2\text{py})]$ with its more sterically hindered base vs $[(\text{CH}(\text{CH}_3)_2\text{Co}(\text{DH})_2 \text{py})]$.^{7d}

To predict a similar trend for cobinamides, and because no X-ray crystal structures of axial bases coordinated to cobinamides are presently available,⁸ molecular modeling was performed on the $[\text{AdoCbi}\cdot\text{bulky base}]^+$ complexes we wished to study using the published universal force field (UFF)⁹ and for the axial bases N-MeIm , 1,2- Me_2Im , py , 2-Mepy, and 2,6- Me_2py . The UFF molecular mechanics results show a similar trend for cobinamides (Table 1); specifically, the sterically hindered base 1,2- Me_2Im is calculated to have a 0.034 Å longer Co-N bond length than N-MeIm , and the sterically hindered bases 2-Mepy and 2,6- Me_2py are calculated to have 0.049 and 0.119 Å longer Co-N bond lengths than py , respectively. From these results, the sterically hindered bases 1,2- Me_2Im , 2-Mepy, and 2,6- Me_2py were chosen for the AdoCbi^+ axial-base K_{assoc} thermodynamic and Co-C bond cleavage product and kinetic experiments reported herein.¹⁰

(5) (a) Part 3: Sirovatka, J. M.; Finke, R. G. *J. Am. Chem. Soc.* **1997**, *119*, 3057. (b) One referee for the present paper questioned the $\text{N-MeIm } K_{\text{assoc}}$ values in our earlier paper.^{5a} Specifically, the referee wondered why the K_{assoc} (110 °C) value obtained from the slope and intercept of the $1/k_{\text{obs}}$ vs $1/[\text{base}]$ plot (see eq 1 and Figure 4 elsewhere^{5a}) does not appear to be the same as the extrapolated K_{assoc} (110 °C) from the ΔH and ΔS values generated by the thermodynamic studies (Table 1 elsewhere^{5a}). It turns out that that the K_{assoc} (110 °C) value from the $1/k_{\text{obs}}$ vs $1/[\text{base}]$ plot, $1.4 \pm 1.6 \text{ M}^{-1}$ (at 2σ error bars) is known to be less accurate than the extrapolated K_{assoc} (110 °C) $\cong 0.02 \text{ M}^{-1}$ generated from the independently measured thermodynamic ΔH and ΔS values. Also, because we know K_{assoc} (50 °C) = $0.18 \pm 0.03 \text{ M}^{-1}$ and the negative ΔH value for the axial-base association ($-7.8 \pm 0.4 \text{ kcal/mol}$), it follows that K_{assoc} (110 °C) must be $\leq 0.18 \text{ M}^{-1}$. Hence, we simply chose the more accurate, independently measured K_{assoc} (110 °C) $\cong 0.02 \text{ M}^{-1}$ to obtain the final deconvoluted $k_{\text{on,h}}$ and $k_{\text{on,het}}$ that we reported.^{5a} Note, however, that the level of agreement in K_{assoc} is dependent on the particular base and the quality of the data each base allows. For example, previous data for $\text{Me}_2\text{N-py}$ from the $1/k_{\text{obs}}$ vs $1/[\text{base}]$ plot yielded a K_{assoc} (110 °C) = $0.6 \pm 0.1 \text{ M}^{-1}$, in nice agreement with the value measured independently from the thermodynamic experiments, K_{assoc} (110 °C) = 0.5 ± 0.2 .^{4b}

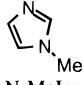
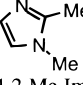
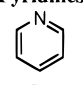
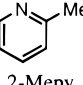
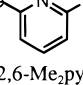
(6) (a) These calculations, using a simplified Me-Co-NH_2 trans-axial base B_{12} model ligand system, predict that at short Co-N (axial) bond lengths, σ effects favor Co-C heterolysis, whereas longer Co-N (axial) bond lengths will favor Co-C bond homolysis. The MO calculations in question use a NH_2 ligand to model the nitrogenous axial base, which, although necessary for these MO calculations, models *only* σ effects, the $-\text{NH}_2$ ligand lacking any π orbitals. (b) Mealli, C.; Sabat, M.; Marzilli, L. G. *J. Am. Chem. Soc.* **1987**, *109*, 1593.

(7) (a) The following Co-N (axial-base) bond lengths have been reported for cobaloximes: 1- $\text{MeImCo}(\text{DH})_2\text{Me}$ [2.058(4) Å], $\text{pyCo}(\text{DH})_2\text{Me}$ [2.068(3) Å], 1,2- $\text{Me}_2\text{ImCo}(\text{DH})_2\text{Me}$ [2.086(1) Å],^{7b} $\text{pyCo}(\text{DH})_2\text{-Pr}$ [2.099(2) Å],^{7c} 1,2- $\text{Me}_2\text{ImCo}(\text{DH})_2\text{-Pr}$ [2.121(2) Å],^{7d} 2- $\text{NH}_2\text{pyCo}(\text{DH})_2\text{-Pr}$ [2.194(2) Å].^{7c} (b) Pahor, N. B.; Attia, W. M.; Geremia, S.; Randaccio, L. *Acta Crystallogr.* **1989**, *C45*, 561. (c) Summers, M. F.; Toscano, P. J.; Bresciani-Pahor, N.; Nardin, G.; Randaccio, L.; Marzilli, L. *J. Am. Chem. Soc.* **1983**, *105*, 6259. (d) Pahor, N. B.; Randaccio, L.; Zangrando, E. *Inorg. Chim. Acta* **1990**, *168*, 115.

(8) White, W. T.; Finke, R. G. Experiments in progress.

(9) (a) Rappé, A. K.; Casewit, C. J.; Colwell, K. S.; Goddard, W. A., III; Skiff, W. M. *J. Am. Chem. Soc.* **1992**, *114*, 10024. (b) Casewit, C. J.; Colwell, K. S.; Rappé, A. K. *J. Am. Chem. Soc.* **1992**, *114*, 10035. (c) Casewit, C. J.; Colwell, K. S.; Rappé, A. K. *J. Am. Chem. Soc.* **1992**, *114*, 10046. (d) Rappé, A. K.; Colwell, K. S.; Casewit, C. J. *Inorg. Chem.* **1993**, *32*, 3438.

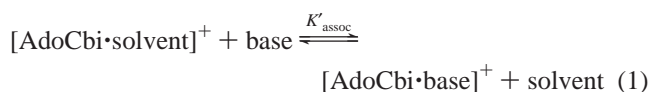
Table 1. Molecular Modeling Co–N(Axial-Base) Bond Distances and Experimentally Determined K_{assoc} Values for [Cbi•Bulky Base]⁺ Complexes Arranged by Axial-Base Category^a

Base	pK _a	AdoCo(III) Cbi- N(axial- base) (Å) ^c	Co(III) Cbi- N(axial- base) (Å) ^c	K_{assoc} (M ⁻¹) (25 °C)
Imidazoles	7.33	2.098	2.090	0.5(1) ^d
				
N-MeIm				
	7.85	2.132	2.129	≤0.007
1,2-Me ₂ Im				
Pyridines	5.29	2.114	2.111	1.0(1) ^d
				
Py				
	5.96	2.163	2.150	≤0.03
2-Mepy				
	6.62	2.233	2.193	≤0.03
2,6-Me ₂ py ^b				

^a [AdoCbi•1,2,4-Me₃Im]⁺ was also modeled, with a resulting AdoCo^{III}–N bond length of 2.19 Å, but was not used for the experimental studies for reasons noted elsewhere.¹⁰ ^b Note that the pyridine ring in the minimized structure for [AdoCbi•2,6-Me₂py]⁺ is no longer perpendicular to the corrin plane; it lies along the north–south axis of the corrin (the line separating the A and C rings from the B and D rings in the corrin, and passing through the cobalt atom), and is bent at an angle of ~15° (from perpendicular) toward the C10 atom in the corrin plane, a conformation that allows coordination of the bulky 2,6-Me₂py. This unusual conformation may, however, be caused by the fixed 0.5 bond length. ^c Only the trends, and not the absolute values, of these estimated distances are believed to be reliable. ^d Taken from our earlier work.^{4a,5}

AdoCbi⁺ Plus Base K_{assoc} Studies. K_{assoc} measurements (upper limits) for each of the bulky base analogues were carried out exactly as done previously with use of visible spectroscopy.^{4a,5a} As we anticipated, none of the sterically hindered bases studied bound to AdoCbi⁺ at 25 °C to any detectable degree using even the highest concentrations of base experimentally possible (2.0 M, Supporting Information, Figures S1–S5). In addition, AdoCbi⁺ was titrated with concentrations of 1,2-Me₂Im up to 7.2 M and at 15 °C to enhance the probability of detecting axial-base binding, but still no [AdoCbi•bulky base]⁺ complex was detected. Upper limits of 0.03 M⁻¹ could, however, be assigned to K_{assoc} values for the nonbinding bases by use of eqs 1 and 2, and by assuming that a minimum of 5% binding of the axial base at the highest concentration of base used could be detected (4% binding is readily detected for [AdoCbi•N-MeIm]⁺).^{5a} $K_{\text{assoc}} \leq [\text{AdoCbi}\cdot\text{base}]^+ / \{[\text{AdoCbi}] \times [\text{base}]\} = 5 \times 10^{-6} / \{[9.5 \times 10^{-5}] \times [2.0]\}$; that is, $K_{\text{assoc}} \leq 0.03$.¹¹ For 1,2-Me₂Im, the upper limit estimate for K_{assoc} can similarly be set at 0.007 M⁻¹ because of the higher concentration of base used. Note that these axial-base binding K_{assoc} values in solution are for the displacement of an axial ethylene glycol solvent molecule, eq 1, the cosolvent bond dissociation energy in [AdoCbi•solvent]⁺ having been

estimated as ca. 8 kcal/mol.^{5a,12}



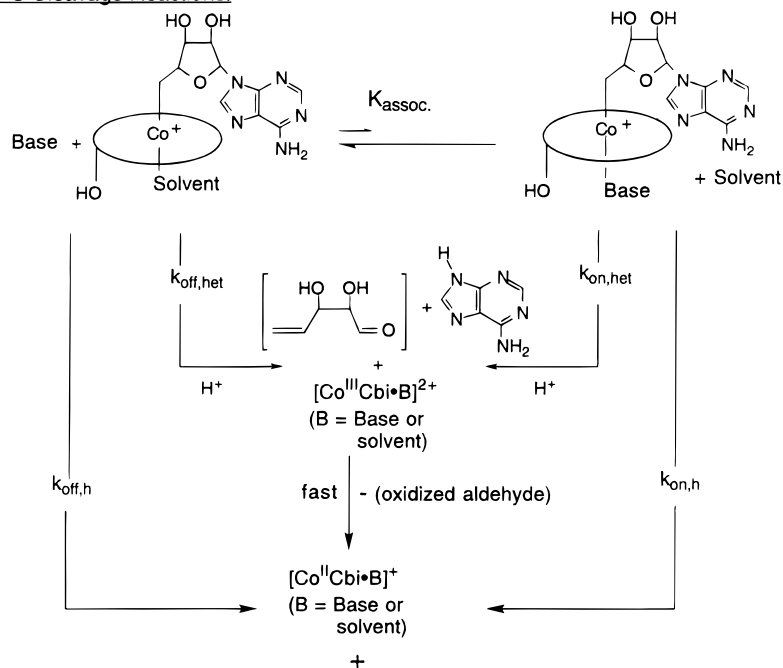
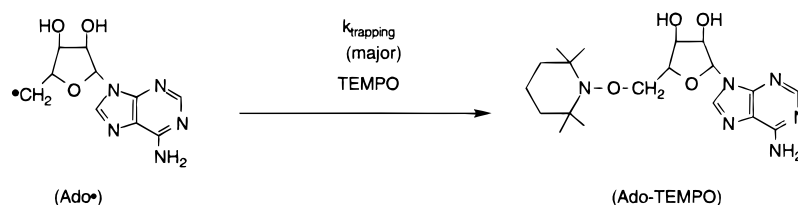
$$K_{\text{assoc}} = \frac{K'_{\text{assoc}}}{[\text{solvent}]} = \frac{[\text{AdoCbi}\cdot\text{base}]^+}{[\text{AdoCbi}]^+ \cdot [\text{base}]} \quad (2)$$

The key result of these axial-base K_{assoc} studies is the following: because the sterically hindered bases do not bind detectably to AdoCbi⁺, there is no detectable change in the ground-state free-energy for [AdoCbi•ethylene glycol]⁺ even in the presence of ≥2.0 M added, sterically bulky base.

[AdoCbi•Bulky Base]⁺ Co–C Thermolysis Product Studies. The products of Co–C bond cleavage [as monitored by high-performance liquid chromatography (HPLC)] are the same as established earlier^{4b,5a,13} for parallel pathways of Co–C homolysis (to Ado-TEMPO) and Co–C heterolysis (to adenine and an adenine byproduct) (Scheme 1). The proton shown in the Co–C heterolysis pathways in Scheme 1 comes from the glycol solvent and is required for adenine formation (as discussed in detail elsewhere^{4b}).¹⁴ Note that the only final cobalt product is Co^{II}Cbi⁺ (100 ± 10%) because of the well-known, fast follow-up reactions at 110 °C that reduce any initially formed Co^{III} to Co^{II} (Scheme 1).^{4b,5a,15}

- Note that this K_{assoc} estimate also makes the assumption that the extinction coefficients for cobinamides with bound sterically hindered bases would be similar to those of [AdoCbi•N-MeIm]⁺ or [AdoCbi•py]⁺, depending on the sterically hindered base used. However, even an unexpected 50% or larger change in the extinction coefficients would not change the key, predicted, and physically reasonable result: the sterically bulky bases do not bind well to AdoCbi⁺.
- Because the λ_{max} of AdoCbi•imidazole in MMCoA mutase is 525 nm,^{12a} that is a red, base-on, and not a yellow, base-off, spectrum is observed, it is clear that the axial histidine in the enzyme is sufficient to provide a “base-on” spectrum. This certainly raises the issue of whether the (solution) $\lambda_{\text{max}} = 525$ nm form is the same, or different, than the solid-state X-ray structure Co–N(Im) distance of ~2.5 Å (they are certainly different in that the X-ray structure is of a form with significant Co^{II}, as well as Co^{III}, present). The Co^{II}Cbi EPR spectrum in MMCoA mutase, and using ¹⁵N-labeled histidine, does show Co^{II}–¹⁵N hyperfine splitting.^{12b} In short, in the MMCoA mutase•AdoCbi•imidazole system, the solution spectroscopic evidence requires that a bond exists between Co and the side-chain imidazole. However, if the solution spectroscopically characterized form of MMCoA mutase has anything like the ~2.5 Å Co–N bond length found in the form of MMCoA mutase characterized by crystallography, then it is relatively weak,^{12c} because it is a Co–N bond length up to ca. 0.2 Å longer Co–N bond than the calculated Co–N bond lengths in any of the [AdoCbi•bulky base]⁺ systems examined herein. (a) Padmakumar, R.; Padmakumar, R.; Banerjee, R. *Biochemistry* **1997**, *36*, 3713. (b) Padmakumar, R.; Taoka, S.; Padmakumar, R.; Banerjee, R. *J. Am. Chem. Soc.* **1995**, *117*, 7033. (c) In this regard it is interesting to note that there is no solvent molecule to displace in AdoCbi; that is, the 5,6-dimethylbenzimidazole apparently serves as a cobalt “protecting group”, one in which the B₁₂ cofactor is protected against solvent coordination until it is at the (presumably H₂O-solvent-free) active site. This, then, would be a way the enzyme can produce a Co–N(imidazole) bond that is even weaker than the estimated bond strength of a solvent molecule coordinated to cobalt, ca. 8 kcal/mol.^{5a}
- Previously, we stated (see p 3058 elsewhere^{5a}) that the 2,3-dihydroxy-4-pentenal product had never been identified unequivocally, but this is in error; Hogenkamp and Barker^{13b} identified it in 1961. (b) Hogenkamp, H. P. C.; Barker, H. A. *J. Biol. Chem.* **1961**, *236*, 3097.
- A referee suggested that using a polar aprotic solvent could lower the amounts of abiological heterolysis (cobalamins are soluble in water and lower alcohols, but are also soluble dipolar aprotic solvents such as dimethyl sulfoxide). Although this is true, the use of a nonprotic solvent would have masked the subtle effects the axial base has on the competing Co–C homolysis vs heterolysis; hence, the use of a protic solvent is deliberate.
- Hay, B. P.; Finke, R. G. *J. Am. Chem. Soc.* **1986**, *108*, 4820.

(10) Because the modeled Co–N bond length for 1,2,4-Me₃Im base falls between that of 2-Mepy and 2,6-Me₂py, 1,2,4-Me₃Im was judged unnecessary for, and thus was not used in, the experimental studies.

Scheme 1. Minimum, Precedented^{4b} Mechanism for AdoCbi⁺ Co–C Bond Cleavage in the Presence of Exogenous Axial-Bases^a**Initial Co–C Cleavage Reactions:****Follow-up Reactions of Ado•**

^a This mechanism is fully supported by, and explains, all our previous results^{4b,5a} and the results presented herein. It faithfully explains *both* the k_{obs} vs [base] plots seen herein (when $K_{\text{assoc}}\cdot[\text{base}] \ll 1$) and the $1/k_{\text{obs}}$ vs $1/[\text{base}]$ seen earlier^{5a} (when $K_{\text{assoc}}\cdot[\text{base}] \geq 0.15$).

Table 2. Kinetic and Product Distribution Results for $[\text{AdoCbi}\cdot\text{bulky base}]^+$ Co–C Bond Thermolysis at 110 °C in Ethylene Glycol with 0.3 M Base Arranged by Axial-Base Category

exogenous base	% total products (mass balance)	% homolysis ^a	% heterolysis ^b	$k_{\text{obs}} \times 10^5 \text{ s}^{-1}$ (110 °C)	$k_{\text{on,h}}$ (s^{-1}); experimental value (or estimated lower limit)	$k_{\text{on,het}}$ (s^{-1}); experimental value (or estimated lower limit)
none (AdoCbi ⁺ •solvent)	100	98	2	0.32 (0.10)	NA ^c $k_{\text{off,h}} = 3.2(1.0) \times 10^{-6}$	NA ^c $k_{\text{off,het}} = 8(3) \times 10^{-8}$
imidazoles						
N-MeIm ^d	100	52	48	3.4(2)	$2.8(5) \times 10^{-3}$	$2.4(5) \times 10^{-3}$
1,2-Me ₂ Im	99	8	91	4.3(3)	$\geq 1.5 \times 10^{-3}$	$\geq 1.8 \times 10^{-2}$
pyridines						
Py ^d	101	94	7	0.46(9)	$7.5(2.6) \times 10^{-4}$	$4(1) \times 10^{-5}$
2-Mepy	102	78	24	1.0(1)	$\geq 5.8 \times 10^{-4}$	$\geq 1.7 \times 10^{-4}$
2,6-Me ₂ py	98	92	6	0.89(5)	$\geq 5.9 \times 10^{-4}$	$\geq 4.1 \times 10^{-5}$

^a To Ado-TEMPO, the only homolysis product detected. ^b To adenine and the preceded adenine byproduct^{5a} formed by a degradation reaction with the added exogenous base. ^c Not applicable, because of the absence of an exogenous nitrogen base. ^d Taken from our earlier work.^{5b,6a}

The product studies (Table 2) show a large range for the amount of heterolysis, observed as a function of the added, exogenous, axial base: for imidazoles, N-MeIm gives 50% heterolysis, while 1,2-Me₂Im gives 91% heterolysis. This record amount of Co–C heterolysis by 1,2-Me₂Im, despite its *predicted longer* Co–N(axial-base) bond, was not anticipated; hence, this result was rechecked carefully. It is experimentally reproducible. For the pyridine bases, py gives 7% heterolysis, 2-Mepy gives 24% heterolysis, and 2,6-Me₂py gives 6% heterolysis. *In short, the data reveal no simple trend for the percent heterolysis or*

homolysis for the pyridine bases and as a function of the predicted bond length. Also, the record amount of heterolysis when 1,2-Me₂Im is the added base is contrary to the predictions of molecular orbital calculations cited in the introduction which considered σ effects only.⁶

The main conclusions here are clear: (i) no simple correlation exists between the ground-state Co–N(axial-base) bond length and the amount of heterolysis or homolysis, and (ii) imidazoles are unusual in their effects on Co–C homolysis vs heterolysis. We previously noted^{5a} that one preceded¹⁶ difference between

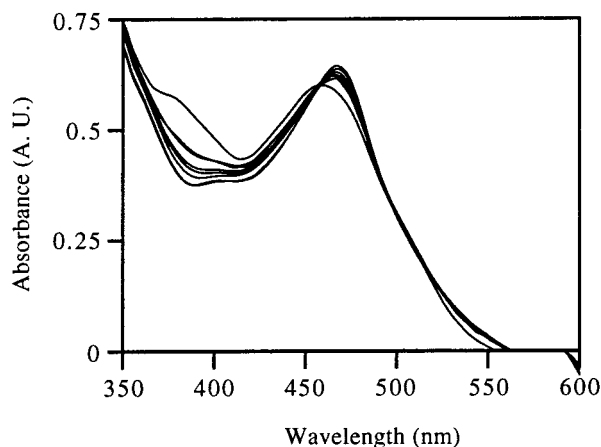


Figure 2. Visible spectra of the thermolysis of $\sim 1 \times 10^{-4}$ M AdoCbi⁺ with 0.3 M 2,6-Me₂py at 110 °C in ethylene glycol, exhibiting an isosbestic point at 460 nm (and 340 nm; not shown).

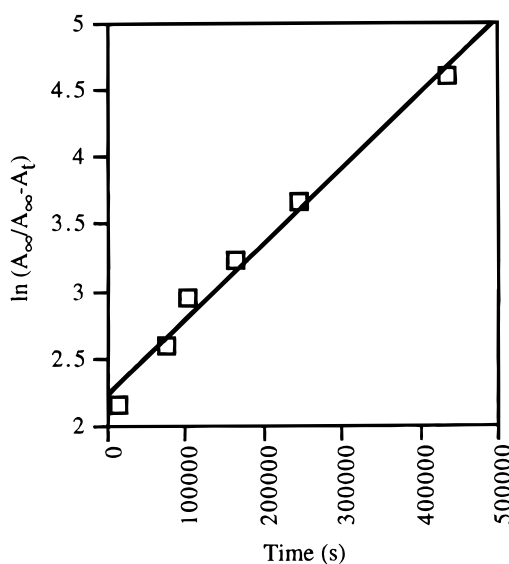


Figure 3. $\ln(A_{\infty}/(A_{\infty} - A_t))$ vs time plot of the thermolysis of $\sim 1 \times 10^{-4}$ AdoCbi⁺ with 0.3 M 2,6-Me₂py at 110.0 °C in ethylene glycol.

imidazoles compared to pyridines, for example, is that imidazoles have a greater capability for both σ and π interactions with metals.

[AdoCbi·Bulky Base]⁺ Co–C Thermolysis Kinetic Studies. The visible spectra data (Figure 2; Supporting Information, Figures S11, S13, S15, S17, and S19) can be fit to first-order $\ln[A_{\infty}/(A_{\infty} - A_t)]$ vs time plots at 474 nm yielding a value for k_{obs} for each base, Figure 3 (plots are provided in Supporting Information, Figures S12, S14, S16, S18, and S20).

The fact that the products of [AdoCbi·bulky base]⁺ thermolysis are closely analogous to those from [AdoCbi·nonhindered base]⁺ allows one to adopt, as an initial working mechanistic hypothesis, the previously established^{4b,5a} mechanism for [AdoCbi·base]⁺ thermolyses (Scheme 1). This mechanism, in turn, yields the rate law shown in eq 3, from which the relationship between k_{obs} and [base] in eq 4 can be derived. In addition, because $K_{\text{assoc}} \leq 0.03 \text{ M}^{-1}$ and hence $K_{\text{assoc}} \cdot [\text{base}]$

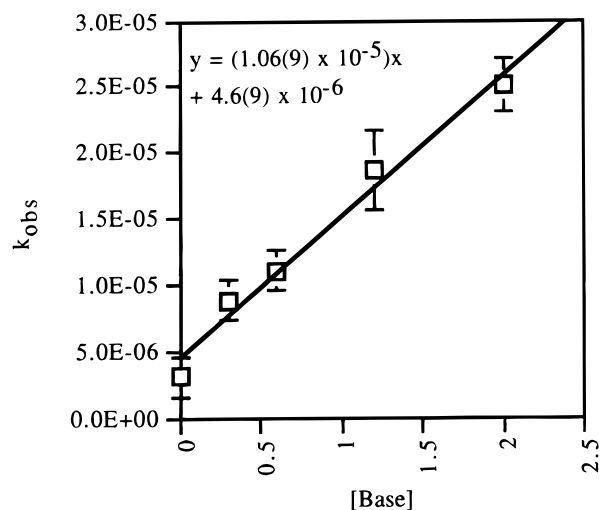


Figure 4. k_{obs} vs [2,6-Me₂py] plot for the rates of thermolysis of $\sim 1 \times 10^{-4}$ AdoCbi⁺ with 0–2.0 M 2,6-Me₂py at 110.0 °C in ethylene glycol.

is $\ll 1$ for all cases studied herein, eq 4 can be simplified to eq 5, which predicts a linear k_{obs} vs [base] relationship.

$$\frac{d[\text{Co}^{\text{II}}\text{Cbi}^+]}{dt} = \frac{d[\text{AdoCbi}^+]}{dt} k_{\text{off,h}}[\text{AdoCbi}^+] + k_{\text{off,het}}[\text{AdoCbi}^+] + k_{\text{on,h}}[\text{AdoCbi}^+ \cdot \text{base}] + k_{\text{on,het}}[\text{AdoCbi}^+ \cdot \text{base}] \quad (3)$$

$$k_{\text{obs}} \equiv \frac{k_{\text{off,T}} + k_{\text{on,T}} \cdot K[\text{base}]}{1 + K[\text{base}]} \quad (4)$$

$$k_{\text{obs}} = k_{\text{off,T}} + k_{\text{on,T}} \cdot K[\text{base}] \quad (5)$$

Experimentally, a linear plot of k_{obs} vs [base] for 2,6-Me₂py is observed (Figure 4); a plot for 1,2-Me₂Im gave an analogous linear k_{obs} vs [1,2-Me₂Im] plot and is provided in the Supporting Information (Figure S25). The ability of the mechanism in Scheme 1 to rationalize both the present linear k_{obs} vs [base] plots, as well as the earlier, linear $1/k_{\text{obs}}$ vs $1/[\text{base}]$ plots (for the case of $K_{\text{assoc}} \cdot [\text{base}] \geq 0.15$),^{5a} is strong evidence for its validity and broader applicability.

A further test of the mechanism in Scheme 1 is the prediction that the product ratio will be constant throughout the reaction, $[\text{product ratio}]_T \equiv [\text{adenine}]_T/[\text{Ado} \cdot \text{products}]_T = k_{\text{on,het}}/k_{\text{on,h}}$ (eq 8a, Supporting Information). Experimentally, the Co–C homolysis-to-heterolysis product ratio is indeed constant over time within the observed experimental error for both the nonbulky base N-MeIm, and also for the sterically hindered base 1,2-Me₂Im [N-MeIm product ratios = 1.1(2) at 2.8 h, 1.0(2) at 5.3 h, and 1.0(2) at 24 h; 1,2-Me₂Im product ratios = 16(3) at 2.25 h, 11(2) at 4.5 h, 10(2) at 24 h]. Intuitively, a constant product ratio makes sense as well, because all that it requires is (a) a rapid preequilibrium (K_{assoc} , Scheme 1), and (b) that the ratio of $[\text{AdoCbi} \cdot \text{bulky base}]^+ / [\text{AdoCbi} \cdot \text{solvent}]^+ = K_{\text{assoc}} \cdot [\text{base}]$ be constant throughout the reaction. The rapid preequilibrium for AdoCbl is well-known^{4,5a} [adenosylcobalamin having been reported as “astonishingly labile”¹⁷ for a Co^{III} center], and our choice of [base] = 0.3 M, a 3000-fold excess over [AdoCbi⁺], ensures the second condition for a constant product ratio, $K_{\text{assoc}} \cdot [\text{base}] = \text{constant}$, also be true.

(16) (a) Al-Jaff, G.; Silver, J.; Wilson, M. T. *Inorg. Chim. Acta* **1990**, *176*, 307. (b) Scheidt, W. R.; Chipman, D. M. *J. Am. Chem. Soc.* **1986**, *108*, 1163. (c) Rohmer, M.-M.; Strich, A.; Veillard, A. *Theor. Chim. Acta (Berlin)* **1984**, *65*, 219. (d) Hoffmann, R.; Howell, J. M.; Rossi, A. R. *J. Am. Chem. Soc.* **1976**, *98*, 2484.

(17) Thusius, D. *J. Am. Chem. Soc.* **1971**, *93*, 2629.

The linear dependence of the kinetics on [2,6-Me₂py] seen in Figure 4, and the well-known fact that kinetics reveals the composition of the activated complex of the rate-determining step,¹⁸ yield the important result that the sterically bulky bases (1,2-Me₂Im, 2-Mepy, and 2,6-Me₂py) *must be involved in the rate-determining Co–C bond cleavage step*. In addition, the data in Figure 4 serve as a useful control for this work: the intercept, $k_{\text{off},T}$, is $4.6(9) \times 10^{-6} \text{ s}^{-1}$, the same within experimental error as the value of $k_{\text{off},T}$ determined independently ($k_{\text{off},T} = 3(1) \times 10^{-6} \text{ s}^{-1}$).^{4b} This serves as a further check of the mechanism, its associated kinetic derivation, eqs 3–5, and the metrical analysis of the data. Because there is no detectable change in the ground-state free energy (no nonkinetically detectable axial-base binding, and thus no detectable ground-state stabilization or destabilization), yet the kinetics proves that the sterically bulky axial bases are involved in the rate-determining step, it follows that all of the Co–C cleavage in fact occurs from a low-level amount of the base-on form, [AdoCbi•bulky base]⁺. This result, the fact that the K_{assoc} for the bulky bases is immeasurably small ($\leq 0.03 \text{ M}^{-1}$) yet the bulky bases *do* bind to Co^{II}Cbi⁺ (vide infra), requires that the dominant effect of the bulky axial base is at the Co–C cleavage transition state $\{[\text{Ado} \cdots \text{CoCbi} \cdot \text{bulky base}]^{\ddagger}\}$.

In our previous studies, the independently determined K_{assoc} values allowed deconvolution of the data into the individual $k_{\text{on,h}}$ and $k_{\text{on,het}}$ rate constants.^{5a} However, in the current work, and because only an upper limit to K_{assoc} can be estimated, one can obtain only lower-limit estimates for the values of $k_{\text{on,h}}$ and $k_{\text{on,het}}$ by using the estimated *upper* limit for K_{assoc} at 25 °C (Table 1) as the upper limit for K_{assoc} at 110 °C. [Previously we showed that the K_{assoc} values decrease with increasing temperature because axial-base binding is exothermic;^{4b,5a} hence, the inequality that $K_{\text{assoc}}(25 \text{ °C}) \gg K_{\text{assoc}}(110 \text{ °C})$ is almost surely valid.] Substituting this upper limit for K_{assoc} and the known values for $k_{\text{off},T}$ ^{4b} into eq 5 gives the lower limit for $k_{\text{on},T}$. Then, putting the lower-limit value for $k_{\text{on},T}$ into eq 8a (Supporting Information) allows one to use the constant heterolysis-to-homolysis product ratio obtained by HPLC to derive lower-limit estimates for $k_{\text{on,h}}$ and $k_{\text{on,het}}$ (Table 2); specifically, $k_{\text{on,h}} \geq 1.5 \times 10^{-3} \text{ s}^{-1}$ and $k_{\text{on,het}} \geq 1.8 \times 10^{-2} \text{ s}^{-1}$ for [AdoCbi•1,2-Me₂Im]⁺. These values, compared with those for [AdoCbi•solvent]⁺ in Table 2, $k_{\text{off,h}} = 3.2 \times 10^{-6} \text{ s}^{-1}$ and $k_{\text{off,het}} = 8 \times 10^{-8} \text{ s}^{-1}$, permit one to calculate the accelerations of Co–C homolysis, ≥ 470 -fold, and heterolysis, $\geq 2 \times 10^5$ -fold, for [AdoCbi•1,2-Me₂Im]⁺. The $\geq 2 \times 10^5$ acceleration of Co–C *heterolysis* induced by 1,2-Me₂Im is a new record, one apparently occurring despite the expectation of a longer Co–N(axial-base) bond.

The acceleration of Co–C *homolysis* of ≥ 470 -fold is almost surely (and despite the inequality²⁰) only a fraction of the 10¹² enzymic acceleration (10¹⁴ if one uses [AdoCbi•solvent]⁺ rather than AdoCbl as the comparison point^{21c})—that is, there is no evidence for 1,2-Me₂Im being able to accomplish anything like

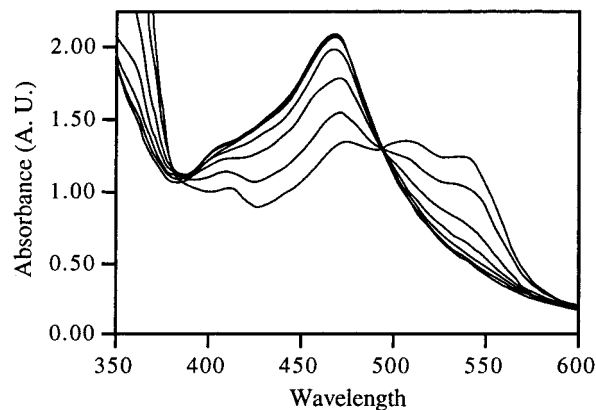


Figure 5. Visible spectra of the titration of $\sim 1 \times 10^{-4} \text{ Co}^{\text{II}}\text{Cbi}^+$ with 2,6-Me₂py at 25 °C. The lack of a clean isosbestic point at 380 nm is most likely due to base binding at both the α and β sides of the corrin ring, resulting in a three-species equilibrium.

the 10^{12–14} acceleration¹⁹ of Co–C homolysis, and in fact there is now chemical precedent against it.

Co^{II}Cobinamide Plus Sterically Hindered Axial-Base Binding Studies. Hammond's postulate²¹ allows one to model the axial-base effect on the Co^{II}-component of the [Ado••••Co^{II}]⁺ endothermic (by $\approx 30 \text{ kcal/mol}$ ^{21c,22}) Co–C homolysis transition state by examining the interaction of base with the Co^{II}Cbi⁺ product. The spectra of Co^{II}Cbi⁺ with added base (1,2-Me₂Im, 2-Mepy, and 2,6-Me₂py) show that the sterically hindered bases used in this study *do bind* to Co^{II}cobinamide, as the kinetic studies indirectly predict, and even though there is no *detectable* ground-state binding to AdoCo^{III}cobinamide (see Figure 5; Supporting Information, Figures S7–S10). However, isosbestic points were not seen, and no linear plots were obtained when analyzing the spectra (using eq 6 in the Experimental Section). These results imply that a ≥ 3 species system is present, almost surely because of bulky base binding to both the α and β sides of the corrin, the β side now being open in Co^{II}Cbi⁺. (The [Ado••••Co^{II}]⁺ homolysis transition state of course involves only the α -bound [AdoCbi•bulky base]⁺, because the Ado group occupies the β -axial position.) Hence, quantitative $K_{\alpha,\text{assoc}}$ and $K_{\beta,\text{assoc}}$ values for [Co^{II}Cbi•bulky base]⁺ complexes remain to be determined. The key result, nevertheless, is still clear: these results confirm the finding from the kinetics that the sterically hindered axial bases bind best to, and thus exert a stronger control on, the energetics of the *Co^{II}-like transition-state for the Co–C homolysis reaction*. Noteworthy here is the paucity of [Co^{II}Cbi•base]⁺ X-ray structural studies,^{21b} a gap in the Co(corrin) structural literature which needs to be filled.

The thermodynamic and kinetic results yield a similar conclusion for the [Co^{III}••••Ado]⁺ heterolysis transition state (i.e., and the dominance of axial-base effects at the Co–C heterolysis transition state). Again, a search of the X-ray crystallographic literature²³ reveals a lack of [Co^{III}Cbi•bulky base]²⁺ structures.

(18) Espenson, J. H. *Chemical Kinetics and Reaction Mechanisms*; McGraw-Hill: New York, 1981; p 90.

(19) Finke, R. G.; Hay, B. P. *Inorg. Chem.* **1984**, *23*, 3041.

(20) (a) We only have a lower-limit estimate of $k_{\text{on,h}}$ ($\leq 1.5 \times 10^{-3} \text{ s}^{-1}$ for 1,2-Me₂Im) and $k_{\text{on,het}}$ ($\leq 1.8 \times 10^{-2} \text{ s}^{-1}$ for 1,2-Me₂Im); hence, the true acceleration of Co–C bond cleavage caused by the bulky bases is rigorously unknown. However, preliminary K_{assoc} results^{20b} for [MeCbi•bulky base]⁺ reveal that the K_{assoc} value for [MeCbi•1,2-Me₂Im]⁺ is 14-fold smaller than the K_{assoc} value for [MeCbi•N-MeIm]⁺. Assuming that MeCbi⁺ and AdoCbi⁺ bind sterically hindered bases with K_{assoc} values of the same order of magnitude, then the lower limit rate constants provided herein should give a reasonable estimate (e.g., within 1 to 2 orders of magnitude) for the unknown, exact rate constant values. (b) Sirovatka, J. M.; Finke, R. G. Unpublished results.

(21) (a) Lowry, T. H.; Richardson, K. S. *Mechanism and Theory in Organic Chemistry*; Harper and Row: New York, 1987; pp 212–214. (b) The applicability of Hammond's postulate to the AdoCbl Co–C homolysis event, and the need for [Co^{II}Cbi•base]⁺ structural studies, has been noted previously;^{21c} see especially the top left-hand column on p 8018. (c) Hay, B. P.; Finke, R. G. *J. Am. Chem. Soc.* **1987**, *109*, 8012.

(22) Hay, B. P.; Finke, R. G. *Polyhedron* **1988**, *7*, 1469.

(23) (a) Glusker, J. P. In *B₁₂*; Dolphin, D., Ed.; John Wiley and Sons: New York, 1982; Vol. 1, Chapter 2. (b) Rossi, M.; Glusker, J. P. In *Environmental Influences and Recognition in Enzyme Chemistry*; Liebman, J. F.; Greenburg, A., Eds.; VCH: New York, 1988; Vol. 10, Chapter 1.

Attempted Correlations of Product and Kinetic Results with Axial-Base pK_a or with Estimated $\text{Co}^{\text{III}}\text{Cbi}^{2+}$ and $\text{Co}^{\text{II}}\text{Cbi}^+$ (Axial-Base) Bond Lengths. The key insight above, that the dominant axial-base effect is in the Co^{III} and Co^{II} transition states, logically leads one to try to correlate the product ratios and homolysis and heterolysis rates with transition-state properties of the $\text{Co}^{\text{III}}\text{---}$ or $\text{Co}^{\text{II}}\text{---N(axial-base)}$ interaction, such as the $\text{Co}^{\text{III}}\text{---N}$ or $\text{Co}^{\text{II}}\text{---N(axial-base)}$ bond distances. $\text{Co}^{\text{III}}\text{---N(axial-base)}$ bond distances were estimated using molecular modeling by deleting the adenosyl group from the $[\text{AdoCbi}\cdot\text{axial-base}]^+$ model structure and optimizing the geometry as done for the AdoCbi^+ structures.

The estimated Co^{III} bond distances for the axial bases used in this study (Table 1), follow the same trend determined for the $[\text{AdoCbi}\cdot\text{bulky base}]^+$ structures; the $\text{Co}^{\text{III}}\text{---N}$ bond lengths are somewhat shorter (0.003–0.04 Å) than for the analogous, sterically more crowded $[\text{AdoCbi}\cdot\text{bulky base}]^+$ complexes. The key result is the following: *no simple correlation is apparent* if one plots the $\text{Co}^{\text{III}}\text{---N(bulky base)}$ estimated bond lengths vs the amount of homolysis or heterolysis, respectively, or vs the rate constants for homolytic or heterolytic cleavage, respectively (Figures S26, S27, Supporting Information). Moreover, the amount of heterolysis and the rate constants of cleavage were plotted vs the pK_a values of the axial bases, but no simple correlation is apparent here either (Figures S28, S29, Supporting Information). In short, no simple correlation exists between the product ratios or rate constants for $\text{Co}\text{---C}$ bond cleavage and any single characteristic of the axial bases examined.

Because no Co^{II} atom is available within UFF, there is no way at present to model directly the $\text{Co}^{\text{II}}\text{---N(axial-base)}$ bond lengths. [Also, an examination of Co^{III} vs Co^{II} cobalamin crystal structures suggests electronic as well as steric effects on the $\text{Co}\text{---N(axial-base)}$ bond lengths when the oxidation state of cobalt is changed from Co^{III} to Co^{II} .^{24a}] However, a first-order approximation for the $\text{Co}^{\text{II}}\text{---N(axial-base)}$ bond lengths can be readily obtained by adding the increase in ionic radius of Co^{II} vs Co^{III} , 0.12 Å,²⁵ to the $\text{Co}^{\text{III}}\text{---N(axial-base)}$ bond lengths. The key point here is that the $\text{Co}^{\text{II}}\text{---N(axial-base)}$ bond lengths *should follow the same trend* as the $\text{Co}^{\text{III}}\text{---N(axial-base)}$ bond lengths. Hence, once again, no simple correlation is anticipated between the estimated $\text{Co}^{\text{II}}\text{---N(axial-base)}$ bond lengths and any single characteristic of the axial bases examined.

Co–C Cleavage Product and Kinetic Control Studies of $[\text{AdoCbi}\cdot\text{ImH}]^+$ and $[\text{AdoCbi}^+\cdot\text{Im}^-]$. The crystal structure of methylmalonyl-CoA mutase^{2a} shows a histidine side-chain imidazole (ImH) coordinated to the cobalt atom, one possibly partially deprotonated by an aspartate ($-\text{CO}_2^-$) residue. Hence, it is important to compare the results of this study and our earlier work,^{5a} using *N*-methylated imidazoles, with the results obtained in control experiments herein using imidazole itself and the imidazolate anion (i.e., Im^- as the limiting, fully deprotonated, model for the maximum possible effects of any partial deprotonation).

The results show that imidazole gives the same kinetic and product results as *N*-MeIm within experimental error; the rate of $\text{Co}\text{---C}$ bond cleavage with imidazole as an axial base is $k_{\text{obs}} = 3.4(6) \times 10^{-5} \text{ s}^{-1}$ [compared with $3.4(2) \times 10^{-5} \text{ s}^{-1}$ for *N*-MeIm^{5a}], and the amount of homolysis for imidazole is 50-(5)% [compared with 52(5)% for *N*-MeIm^{5a}]. These results demonstrate that *N*-MeIm, chosen for our earlier studies,^{5a} is in fact a suitable replacement for imidazole in solution chemical precedent studies. Actually, the repeatable, nonisobestic points seen in a titration of AdoCbi^+ with added imidazole (Figure S6, Supporting Information) demonstrate the wisdom of choosing *N*-MeIm for our initial imidazole plus axial-base studies,^{5a} a choice made initially^{5a} on the basis of earlier literature (see ref 11h elsewhere^{5a}).

The results of the control experiment using imidazolate, Im^- , a strongly σ -donating base with a predicted short $\text{Co}\text{---N}$ bond length, are very different from those of imidazole itself: complete (105(5)%) heterolysis at 25 °C (no homolysis products were detectable), with $k_{\text{obs}} = 7.37(6) \times 10^{-5} \text{ s}^{-1}$ at 25 °C. The brilliant pink Co^{III} product is also of some interest, presumably $[\text{Co}^{\text{III}}\text{Cbi}^{2+}\cdot(\text{Im}^-)_2]$ or possibly the bridged $[(\text{Im}^-)\text{Co}^{\text{III}}\text{Cbi}^{2+}\cdot\text{Im}^- \cdot \text{Co}^{\text{III}}\text{Cbi}^{2+}(\text{Im}^-)]^+$.²⁶ This product is another interesting candidate for X-ray crystallographic studies.

Previously, only ligands such as cyanide anion^{27,28} have been shown to cause quantitative $\text{Co}\text{---C}$ heterolysis. However, the dominance of $\text{Co}\text{---C}$ heterolysis for Im^- is as expected for this strong σ -donor strength ligand (ImH, $pK_a = 14.7$), given our published finding that strong σ donors induce $\text{Co}\text{---C}$ heterolysis.^{5a}

We also examined the sterically hindered 4-methylimidazolate to see if a longer $\text{Co}\text{---N}$ bond would begin to offset the large σ effects noted for imidazolate. The rate of $\text{Co}\text{---C}$ bond cleavage was 3.2-fold slower, $k_{\text{obs}} = 2.3(1) \times 10^{-5} \text{ s}^{-1}$, but the products are still 100% $\text{Co}\text{---C}$ heterolysis. The results indicate that the large σ effects generated by complete deprotonation are not significantly affected by the estimated slightly longer $\text{Co}\text{---N}$ bond length (~ 0.034 Å by molecular mechanics calculations) generated by 4-methylimidazolate compared with Im^- itself. These imidazolate results certainly confirm that strong σ donors at unrestricted (short) distances give rise to complete $\text{Co}\text{---C}$ heterolysis. (The $\text{Co}\text{---N}$ distance in $[\text{AdoCbi}^+\cdot\text{Im}^-]$ is 2.10 Å by molecular modeling.)

Of interest here are recent biochemical results with glutamate mutase, another imidazole base-on enzyme, which indicate that the histidine–aspartate pair is crucial to catalysis and imply that either the partial deprotonation of histidine, or possibly a fixed conformation of histidine in relation to the corrin ring, may play important roles in the enzymic catalytic cycle.²⁹ The above-mentioned imidazolate chemical precedent results, showing that imidazolate plus AdoCbi^+ produces rapid and complete abiological heterolysis, imply that the histidine in the enzymic system is probably (a) only partially deprotonated and (b) also at a long $\text{Co}\text{---N}$ distance (i.e., longer than that generated by the 4-methylimidazolate control experiment herein). The partial deprotonation at most is, of course, the expected result given the (nonenzymic) pK_a values of the unperturbed residues

(24) (a) Sirovatka, J. M.; Rappé, A.K.; Finke, R. G., manuscript in preparation. Sample results for $\text{Co}\text{---C}$ bond lengths are as follows. AdoCbl : UFF gives 2.07 Å, compared with 2.02 (Brown's MM2) and 2.02(3) (observed in the crystal structure).^{24c} MeCbl : UFF gives 2.01 Å, compared with 1.99 (Brown's MM2) and 1.99(2) (observed).^{24c} These values all fall within limits determined for "good" (0.02 Å) or "fair" (0.08 Å) as defined by Rappé et al.^{9d} (b) From the parameter defined as a "good" fit for modeling vs X-ray crystal structures, one can state that the maximum error one could expect when comparing different model structures is 0.02 Å. (c) Marques, H. M.; Brown, K. L. *J. Mol. Struct. (THEOCHEM)* **1995**, *340*, 97.

(25) Huheey, J. E. *Inorganic Chemistry, Principles of Structure and Reactivity*; Harper and Row: New York, 1972; p 74, Table 3.6, 2nd column, Co^{II} and Co^{III} entries.

(26) Hayward, G. C.; Hill, H. A. O.; Pratt, J. M.; Williams, R. J. P. *J. Chem. Soc. (A)* **1971**, 196.

(27) (a) Brasch, N. E.; Hamza, M. S. A.; van Eldik, R. *Inorg. Chem.* **1997**, *36*, 3216. (b) Pratt, J. M. *Inorganic Chemistry of Vitamin B₁₂*; Academic Press: London, 1972. (c) Johnson, A. W.; Shaw, N. J. *Chem. Soc. A* **1962**, 4608.

(28) CN^- is known to have strong π -acceptor effects in $\text{Co}^{\text{III}}\text{Cbl}$ chemistry. (a) Brown, K. L.; Gupta, B. D. *Inorg. Chem.* **1990**, *29*, 3854. (b) Brown, K. L.; Satyanarayana, S. *Inorg. Chem.* **1992**, *31*, 1366.

(29) Chen, H.-P.; Marsh, E. N. G. *Biochemistry* **1997**, *36*, 7884.

involved, histidine (N-HIm), $pK_a = 6.04$, and aspartate ($-\text{CO}_2^-$), pK_a of the conjugate acid = 3.90.³⁰

Discussion

Key Findings. The key findings from these [AdoCbi•sterically bulky base]⁺ chemical precedent studies are as follows: (1) Sterically bulky bases do not bind detectably to AdoCbi⁺ in the ground state, the estimated upper limit K_{assoc} values for [AdoCbi•bulky base]⁺ all being $\leq 0.03 \text{ M}^{-1}$. Hence, there is no detectable free-energy change to the AdoCbi⁺ ground state in the presence of sterically bulky axial bases. (2) Product studies of the thermolysis of AdoCbi⁺ in the presence of sterically bulky bases show that both homolysis and heterolysis occur, but that there is no simple correlation between the amounts of homolysis or heterolysis and the AdoCbi–N(axial-base) bond length, the Co^{III}–N(axial-base) bond length, the estimated Co^{II}–N(axial-base) bond length, or the pK_a of the axial base. The sterically hindered base 1,2-Me₂Im unexpectedly gives more Co–C heterolysis than N-MeIm (52%), an overall record amount (91%). (3) The kinetic studies demonstrate that the rate of Co–C thermolysis is linearly dependent on the concentration of sterically hindered base, requiring that the bulky bases are involved in the rate-determining Co–C bond cleavage step. (4) Sterically hindered bases *do* bind to Co^{II}Cbi⁺ (as indirectly predicted by the kinetic results), Co^{II}Cbi⁺ being the best available, experimentally accessible energetic model of the [Ado••••Co^{II}Cbi][‡] homolysis transition state. And (5) product studies of [AdoCbi•Im⁻]⁺ and [AdoCbi•4-MeIm⁻]⁺ reveal complete Co–C abiological heterolysis at 25 °C.

Four questions evolve from these data: (a) Why does 1,2-Me₂Im exhibit record amounts of heterolysis? (b) Why is there no simple correlation between the Co–N(axial-base) bond length and the amount of heterolysis or the rates of heterolytic cleavage? (c) What precedent is there for the dominance of transition-state effects in cobalamin (or other biological cofactor) reaction mechanisms? And, (d) what implications do these chemical precedent studies have on B₁₂-dependent enzymatic systems, particularly the ones with the imidazole base-on binding motif? The following discussion attempts to provide plausible answers to these questions or, in some cases, hypotheses that will require further experimental scrutiny.

Distance-Dependent σ and π Effects and Their Influence on Co–C Homolysis vs Heterolysis Product Distributions. The record enhanced heterolysis for 1,2-Me₂Im (91%), the opposite of the MO-based (σ effects only) prediction of *less* heterolysis with a longer Co–N(axial-base) bond,⁶ is worth discussing. We were able to conceive of four alternative explanations for this intriguing result. (1) Deprotonation of ethylene glycol by 1,2-Me₂Im yields HOCH₂CH₂O⁻, and that strongly σ -donating species is responsible for the observed Co–C heterolysis; (2) cage effects are responsible, giving initial homolytic cleavage followed by electron transfer in the caged pair to yield net Co–C heterolysis; (3) steric effects, ones somehow not accurately reported in the modeling calculations, are important; or (4) that *both* σ and π effects are important in controlling Co–C bond homolysis vs heterolysis in a combined, nonlinear function of the Co–N(axial-base) bond length. The first alternative hypothesis was ruled out experimentally, whereas the second is incompatible with the observed kinetics; a full discussion of these first two hypotheses is provided in the Supporting Information.

However, it is conceivable that, according to the third hypothesis, the UFF molecular modeling data are somehow inaccurate; for example, the trend discovered in the Co–N (axial-base) bond lengths could, conceivably, be in error. We believe, however, that this is unlikely, because the bond length trends (a) match what one expects from a traditional steric analysis, and (b) are reproduced in cobaloxime B₁₂-model X-ray structures⁷ (with the same axial bases or axial bases of comparable steric bulk). It is also *conceivable* that the axial base exerts a steric influence on the corrin ring that the UFF molecular mechanics misses, the so-called mechanochemical butterfly effect,^{23a} in which the axial base exerts a steric force on the corrin ring, flexing it upward toward the adenosyl ligand, thereby accelerating Co–C cleavage. However, our UFF molecular modeling did not detect any significant increase in the corrin fold angle. (There is a $\leq 3^\circ$ change in the corrin fold angle between [AdoCbi•bulky base]⁺ and [Co(II/III)Cbi•bulky base]⁺ for all of the axial bases studied in our calculations.) Hence, this conceivable explanation for the 1,2-Me₂Im result is judged unlikely. However, the hypothesis that something is wrong with the molecular mechanics calculations in the present case cannot be unequivocally disproven experimentally until X-ray crystal structures of cobinamide•base complexes are available, especially of [Co^ICbi•bulky bases]⁺ and [Co^{III}Cbi•bulky bases]²⁺; work toward this goal is continuing.⁸

This leaves us, then, with explanation (4), σ and π effects that compete as a function of the Co–N(axial-base) bond distance, as the last way to explain the at first puzzling 1,2-Me₂Im result of 91% Co–C heterolysis. *Actually, all that is required to explain the 1,2-Me₂Im result is to realize the well-accepted fact that σ effects in general diminish less rapidly over longer distances than do π effects.*³¹ As the bond length increases in going from N-MeIm (2.090 Å in the [Co^{III}Cbi•N-MeIm]⁺ model for the Co–C heterolysis transition state; 50% observed heterolysis^{5a}) to 1,2-Me₂Im (2.129 Å; 91% observed heterolysis), homolysis-enhancing π effects^{5a} are expected to attenuate more quickly than σ effects,⁶ resulting in less Co–C homolysis and, thus, predominance of Co–C heterolysis, *exactly as seen*. Hence, the unusual—indeed record—amount of Co–C heterolysis for 1,2-Me₂Im is easily rationalized in hindsight with Co–N distance-dependent, competing σ and π effects at intermediate Co–N(axial-base) bond lengths.

An analogous argument holds for the pyridine ligands, and can be extended to 2,6-Me₂py, where π effects may no longer exist to any significant degree, and the remaining σ effects now control Co–C homolysis (92% homolysis observed for 2,6-Me₂py), in agreement with the σ -only MO studies discussed earlier.⁶

The explanation of competing, distance-dependent σ and π effects is presently the only explanation for these results that readily explains all the data and that does not have at least some evidence against it. This is not to say, however, that further studies are not still needed to further support, or refute, this hypothesis of Co–N distance-dependent, competing σ and π effects. In particular, ab initio MO studies involving σ and π effects in B₁₂ complexes, as well as the [Co^ICbi•bulky base]⁺ and [Co^{III}Cbi•bulky base]²⁺ X-ray structural studies cited above, are needed.

The Dominance of Transition-State Effects in the Co–C Cleavage Reaction. One interesting result from the present work is the finding that axial-base effects at the Co–C cleavage *transition state* are dominant. Because $\Delta G = -RT \ln(K_{\text{assoc}})$ and $K_{\text{assoc}} \leq 0.03$, any ground-state *stabilization* of [AdoCbi•

(30) Voet, D.; Voet, J. G. *Biochemistry*; John Wiley & Sons: New York, 1990; p 62.

(31) Levine, I. N. *Quantum Chemistry*, 4th ed.; Prentice Hall: Englewood Cliffs, NJ, 1991; p 373.

solvent]⁺ caused by the formation of [AdoCbi•bulky base]⁺ must be ≤2.6 kcal/mol at 110 °C. However, it is presently impossible to rule out unequivocally a to-date unprecedented *destabilization* of the ground state caused by bulky-base binding. But, careful consideration of possible Co–C cleavage reaction coordinate diagrams reveals that any such putative ground-state destabilization *does not accomplish acceleration of Co–C cleavage*, because the predominant form in solution, and thus the Δ*G*^o of the adocobinamide reactant, is that of [AdoCbi•solvent]⁺—that is, the observed Δ*G*[‡] is still the difference in free energy between primarily [AdoCbi•solvent]⁺ and the {[Ado–CoCbi]⁺}[‡] Co–C cleavage transition state. Hence, the present work confirms our earlier suggestion^{5a} of the dominance of axial-base transition-state effects on the Co–C cleavage reaction. This conclusion is further fortified by the recent series of ground-state FTIR and resonance Raman studies of cobalamins by Marzilli, Banerjee, Spiro, and others,³² that there is no change in the *ground-state* Co–C force constant when comparing base-on and base-off cobalamins.

Are There Other Examples of Demonstrated Transition-State Effects in Metallocofactor Elementary Steps? We wondered: are there other documented examples of transition-state effects in the reactions—particularly in an elementary reaction step—of any other metallocofactors? A literature search uncovered only one previous study, that by Fife and Przystas,³³ of a zinc complex that serves as chemical precedent for the zinc-requiring enzyme, carboxypeptidase A. That study does demonstrate transition-state stabilization and thus acceleration of a model hydrolysis reaction. However, that Zn²⁺ reaction involves a prior equilibrium mechanism, for which the *K*_{eq} value is not known and therefore was not deconvoluted from the reported rate constant; hence, that study does not demonstrate transition-state stabilization of an *elementary* step. The demonstration in this article of transition-state stabilization in an elementary step of a metallocofactor studied outside the enzymatic system is, therefore, of fundamental interest.

Last, one cannot help but reflect upon the above-mentioned result in light of Linus Pauling's early idea that enzymes accelerate reactions by binding transition states.³⁴ Pauling states: "The only reasonable picture of the catalytic activity of enzymes is that (in) which...[the active site of the enzyme] is closely complementary...to the substrate molecule in a strained configuration."^{34a} Although our understanding of enzymic rate accelerations has expanded beyond this still-preserved idea of Pauling,³⁵ the present studies reveal an example that is fully consistent with Pauling's 1946 hypothesis and, in present day language, is known as "catalysis of an elementary step,"³⁵ *only now in an enzyme-free cofactor*. This is, of course, an expected result if one accepts Pauling's hypothesis, and if evolution operates on both enzymes and enzymic cofactors.³⁶

We conclude with a caveat about chemical precedent studies, such as those presented herein. It is well-known that chemical precedent studies say nothing, *rigorously*, about any B₁₂-dependent enzyme system—they of course cannot, because no AdoCbl-enzyme system has been studied herein.³⁶ Chemical precedent studies do, however, provide an excellent platform from which to view and appreciate the power of Nature and the intricate catalytic machinery of enzyme•cofactor complexes. A main goal of chemical analogue studies is, as others have noted before,³⁷ to provide precedent for the most plausible explanations of chemical phenomena centered about such beautiful and complex metallocofactors, and to help design optimized studies, ones often slower and more difficult, of the enzymes themselves by providing a highly focused list of what questions, issues, and hypotheses should be among the top priorities for enzymatic investigations.³⁸

Experimental Section

Experimental details and methods are identical with those used previously^{4b,5a} except where otherwise noted below.

Chemicals. AdoCbi⁺BF₄[−] was prepared according to our reported procedure (98% pure by HPLC).³⁹ Note that fresh, clean Ce(NO₃)₃•H₂O is crucial for an acceptable yield (50%) in this synthesis; older (~6 months) Ce(NO₃)₃•H₂O reduced our yield 5-fold, to 10%. 1,2-Me₂Im, 2-Me-py, 2,6-Me₂-py, 4-MeIm, N-HIm, and proton sponge were purchased from Aldrich in the highest purity possible and used as received. To verify its purity, the NMR spectrum of 1,2-Me₂Im was obtained: ¹H NMR (CDCl₃, 20 mg/mL, 25 °C) 2.31 (s, 3H), 3.51 (s, 3H), 6.74 (s, 1H), 6.83 (s, 1H). Sodium imidazolate and sodium 4-methylimidazolate were synthesized from imidazole (or 4-methylimidazole) and sodium hydride in THF according to reported methods.⁴⁰ The nitroxide TEMPO (Aldrich, sublimed by the manufacturer, mp 37–39 °C) was stored at 0 °C and used as received. All other materials were obtained as described previously.^{5a}

Instrumentation. All instrumentation is exactly as described previously.^{5a}

Molecular Modeling Studies. Modeling studies were done on an SGI Indigo2 100 MHz computer, using the published UFF developed by Rappé et al.⁹ To verify the validity of model structures in UFF compared with crystal structures and Marques and Brown's^{24c} modified MM2 force field for corrins, several controls were completed before use of the UFF molecular mechanics in the present study, controls which will be reported in detail elsewhere.^{24a} Specifically, the crystal structures used by Marques and Brown to parametrize their MM2 force field were minimized using our standard minimizing conditions listed below. The results²⁴ indicate that UFF performs equivalent to Marques and Brown's

- (32) (a) Dong, S.; Padmakumar, R.; Banerjee, R.; Spiro, T. G. *Inorg. Chim. Acta* **1998**, *270*, 392. (b) See also footnote 30 in ref 5a cited as a part of the present study for a complete discussion and other pertinent references. (c) Dong, S.; Padmakumar, R.; Maiti, N.; Banerjee, R.; Spiro, T. G. *J. Am. Chem. Soc.* **1998**, *120*, 9947.
 (33) Fife, T. H.; Przystas, T. J. *J. Am. Chem. Soc.* **1980**, *102*, 7297.
 (34) This concept has been expanded and debated during the past 50 years,³⁵ but Pauling's original hypothesis is still the dominant concept. (a) Pauling, L. *Chem. Eng. News* **1946**, *24*, 1375. (b) Pauling, L. *Nature* **1948**, *161*, 707.
 (35) (a) Albery, W. J.; Knowles, J. R. *Biochemistry* **1976**, *15*, 5627. (b) Albery, W. J.; Knowles, J. R. *Biochemistry* **1976**, *15*, 5631. (c) Knowles, J. R.; Albery, W. J. *Acc. Chem. Res.* **1977**, *10*, 105. (d) Chin, J. *J. Am. Chem. Soc.* **1983**, *105*, 6502. (e) Benner, S. A. *Chem. Rev.* **1989**, *89*, 789. (f) Menger, F. M. *Biochemistry* **1992**, *31*, 5368. (g) Murphy, D. J. *Biochemistry* **1995**, *34*, 4507.

- (36) One can pursue the probable evolution of AdoCbl and B₁₂-dependent enzymes further, thoughts which have led us to a "Speculative, but Unifying Hypothesis for One Unappreciated Role of the Axial-Base," specifically that the histidine base-on form must be important in one or more *subsequent steps in the enzymatic cycle*. The obvious candidate here, in MMCoA mutase, is electron transfer to yield a MMCoA anion, which then rearranges, although this remains to be demonstrated in the enzymatic system itself. Further details are available in the Supporting Information.
 (37) (a) Karlin, K. D. *Science* **1993**, *261*, 701. (b) Holm, R. H. *Acc. Chem. Res.* **1977**, *10*, 427.
 (38) A premier case in point is the ca. 10¹² enzymic acceleration of Co–C homolysis discovered via chemical precedent studies,¹⁹ a topic in which two recent studies of Co–C cleavage in the holoenzyme AdoCbl•ribonucleotide reductase are beginning to reveal some exciting, albeit conflicting, answers as to how this record enzymatic acceleration of a single bond cleavage is accomplished. (a) Stubbe, J.; Licht, S.; Gerfen, G.; Silva, D.; Lawrence, C. *Biofactors* **1995/1996**, *5*, 187. Licht, S. S.; Lawrence, C. C.; Stubbe, J. *Biochemistry* **1999**, *38*, 1234. (b) Brown, K. L.; Li, J. *J. Am. Chem. Soc.* **1998**, *120*, 9466.
 (39) Hay, B. P.; Finke, R. G. *J. Am. Chem. Soc.* **1987**, *109*, 8012.
 (40) Collman, J. P.; Brauman, J. I.; Doxsee, K. M.; Halbert, T. R.; Bunnenberg, E.; Linder, R. E.; LaMar, G. N.; Del Gaudio, J.; Lang, G.; Spartalian, K. *J. Am. Chem. Soc.* **1980**, *102*, 4182.

modified MM2 field, at least for the particular subset of corrins first modeled elsewhere.²⁴

Standard Minimization Conditions. Each structure was built into the force field manually and subjected to 10 cycles of annealed dynamics⁴¹ (0.001–600.0 K with a 10 K step size), and the lowest energy structure from the annealed dynamics was then further minimized under conjugate gradient conditions.

Cobinamide structures were built from a previously minimized structure of adenosylcobalamin. The structure of adenosylcobalamin was built from importing its X-ray diffraction-determined⁴² *x*, *y*, and *z* atomic coordinates, which were then subjected to two complete minimizations using the standard conditions cited above. The cobinamides were then built by deleting the benzimidazole axial base (including the phosphodiester group) and adding hydrogen at the terminal phosphate oxygen. Axial bases were initially drawn in manually, and the Co–N_{ax} bond assigned a bond order of 0.5, the lowest bond order available in the program. The 0.5 bond order was assigned to mimic the actual dative coordination of the Co–N bond as closely as possible; a bond order of 1.0 is too high and shortens the Co–N bond in adenosylcobalamin to an unrealistic 1.954 Å (vs 2.24 Å in the crystal structure⁴²). As a control, adenosylcobalamin was annealed and minimized using a bond order of 0.5; the resulting Co–N bond length (2.11 Å) is closer to the crystal structure value (2.24 Å). The modeling results are detailed in Table 1.

To approximate the structural conditions of the [Ado·---Co][†] Co–C cleavage transition state, molecular mechanics calculations were performed on [Co^{III}Cbi·bulky base]²⁺ complexes. The Co^{III}Cbi²⁺ structures were created by deleting the adenosyl ligand from the (Co^{III}[AdoCbi·bulky base]⁺) structures. The resulting structures were then annealed and minimized via the standard conditions cited above. The Co–N bond lengths for the final [Co^{III}Cbi·bulky base]²⁺ structures were shorter than the initial [AdoCbi·bulky base]⁺ structures: N-MeIm, 0.008 Å; 1,2-Me₂Im, 0.003 Å; py, 0.003 Å, 2-Mepy, 0.013 Å, and 2,6-Me₂py, 0.040 Å. In addition, the corrin ring was folded slightly upward, away from the axial base: N-MeIm, 5°; 1,2-Me₂Im, 7°, py, 4°, 2-Mepy, 6°, and 1,2-Me₂py, 5°. The Co–N(axial-base)–C angles (specifically, the N–C (2-carbon) angle in the axial bases) are: N-MeIm, 127°; 1,2-Me₂Im, 135°, py, 120°, 2-Mepy, 127°, and 1,2-Me₂py, 120°.

K_{assoc} Measurements. Samples of 1 × 10⁻⁴ M AdoCbi⁺ in 4 mL ethylene glycol were titrated with each base, and at [base] values ranging from 0.05 to 2.0 M at 25 °C, analogous to our earlier work.^{5a} The absorbance data at 520 nm were worked up according to the appropriate equations and via Drago's plotting method exactly as detailed previously (see eqs 1 and 2 in our earlier work).^{4a,5a} In addition, one sample of 1 × 10⁻⁴ M AdoCbi⁺ was titrated with 1,2-Me₂Im with concentrations up to 7.2 M at 15 °C in an attempt to detect any [AdoCbi·1,2Me₂Im]⁺ complex. The results, provided in Table 1 (with spectra given in Figures S1–S5, Supporting Information), reveal that none of the sterically hindered bases exhibited detectable binding to AdoCbi⁺.

To verify the reliability of our K_{assoc} data, the values for N-MeIm and py were redetermined as control experiments as part of the present work; the resultant values compare well with our earlier published values: K_{assoc} (N-MeIm) = 0.6(1) (0.5(1), previously)^{5a} and K_{assoc} (py) = 1.2(3) (1.0(2), previously).^{4a}

Product Studies: [AdoCbi·Bulky Base]⁺ Co–C Thermolytic Cleavage in Ethylene Glycol with TEMPO. The product studies were performed exactly as detailed previously:^{5a} solutions of ca. 1 × 10⁻⁴ M AdoCbi⁺, 2 × 10⁻² M TEMPO (or 0.85 M TEMPO, the higher amount used to trap caged pair intermediates),^{4b} and 0.3 M base in 4 mL ethylene glycol were heated at 110.0(2) °C for ~24 h for 1,2-Me₂Im or ~144 h (6 days) for 2-Mepy and 2,6-Me₂py. To ensure that the reaction went to completion, the reaction was observed by UV–visible spectroscopy at 474 nm, where both base-off and base-on Co^{II}Cbi⁺ absorb. The solution was cooled to room temperature after the absorbance value at 474 nm stopped changing to three significant figures. The resulting products were analyzed via HPLC. The results are given in Table 2. The result with 1,2-Me₂Im (~91% heterolysis)

was unusual enough that two controls were done to verify its authenticity: (a) the purity of 1,2-Me₂Im was verified (>95% pure by NMR) and (b) the experiment was repeated twice to verify that the products measured were repeatable and correct; identical results within experimental error were indeed observed in each of the three total experiments.

As a control, the product studies for N-MeIm and py were repeated to test the validity of the present data, and agree well with our earlier results: the heterolysis-to-homolysis product ratio for 0.3 M N-MeIm being 1.1 (compared with 1.0 previously^{5a}) and the product ratio for 0.3 M py being 0.06 (compared with 0.07 previously^{4b}).

The cobalt corrin product, [Co^{II}Cbi]⁺ is 100 ± 10% (λ_{max} = 468 nm,³⁹ ε₄₆₈ = 1.1 × 10⁴ M⁻¹ cm⁻¹). Note that although Co–C bond heterolysis produces Co^{III} initially, it reacts rapidly with the heterolysis product 2,3-dihydroxy-4-pentenal (produced stoichiometrically from the pentose sugar) to give reduced Co(II)cobamide and oxidized organic product.^{4b} Hence, the only corrin product detected is Co^{II}Cbi⁺.

Product Studies Control: Evidence for the Constant Ratio of Heterolysis-to-Homolysis Products. Two predictions of the mechanism in Scheme 1 are that, under conditions of excess [base], and if all of the Co–C cleavage occurs via the base-on form as observed previously,^{4b,5a} the ratio of [AdoCbi·solvent]⁺ to [AdoCbi·bulky base]⁺ will remain constant throughout the reaction, so that (a) the product ratio will also remain constant and (b) be invariant as a function of [base]. This was tested experimentally for both the nonsterically hindered base, N-MeIm, and the sterically hindered base, 1,2-Me₂Im.

A solution of ca. 1 × 10⁻⁴ M AdoCbi⁺, 0.85 M TEMPO, and 0.3 M N-MeIm in 4 mL ethylene glycol was heated at 110.0(2) °C for ~24 h in a Schlenk cuvette wrapped with aluminum foil. At 2.8 and 5.3 h (~25% and ~50% reaction completion), the reaction was stopped by cooling the cuvette in a bath of cold water. The cuvette was then taken into the drybox and an aliquot of the reaction solution removed via an HPLC syringe wrapped in aluminum foil. The cuvette was resealed and returned to the oil bath, and the aliquot was analyzed by HPLC. The product ratio results for the HPLC analyses of N-MeIm are as follows: 2.8 h, 1.1(2); 5.3 h, 1.0(2); 24 h, 1.0(2) with 96% mass balance. The exact experiment was repeated for 1,2-Me₂Im, with aliquots taken at 2.25 and 4.5 h (~25% and ~50% reaction completion). The product ratio results for the HPLC analysis of 1,2-Me₂Im are as follows: 2.25 h, 16(3); 4.5 h, 11(2); 24 h, 10(2) with 95% mass balance.

The product ratio was investigated with 1.8 M 1,2-Me₂Im; the amount of heterolysis [87(5)%] was the same within experimental error as that for the 0.3 M 1,2-Me₂Im run (91(5)%)—that is, there is no detectable change in the product ratio as a function of [base]. The same result was obtained for [2,6-Me₂py] with concentrations ranging from 0.3 to 2.0 M [percent heterolysis was 6(5)% at 0.3 M 2,6-Me₂py and 7(5)% at 2.0 M 2,6-Me₂py].

Product Studies Control: Thermolysis of AdoCbi⁺ with Proton Sponge. One possible hypothesis for the record amount (91%) of Co–C heterolysis observed in the [AdoCbi·1,2-Me₂Im]⁺ system was that the sterically hindered base could be deprotonating ethylene glycol, which would go on to induce heterolysis. This was tested experimentally by using 8.2 × 10⁻⁴ M proton sponge to generate the amount of deprotonated ethylene glycol calculated to be formed in the presence of 0.3 M 1,2-Me₂Im. A solution of ~1 × 10⁻⁴ M AdoCbi⁺, 2 × 10⁻² M TEMPO, and 8.2 × 10⁻⁴ M proton sponge in 4 mL ethylene glycol was heated at 110.0(2) °C for 95 h in a Schlenk cuvette covered with aluminum foil. The products from this reaction were 5% adenine (the heterolysis product) and 95% Ado-TEMPO (the homolysis product). The rate of this reaction was measured to be k_{obs} = 8.5(5) × 10⁻⁶ s⁻¹, 19% of the rate measured with 1,2-Me₂Im. The large discrepancy between the observed products and rate for proton sponge, vs those observed with 1,2-Me₂Im (Table 2), disproves this alternative hypothesis as to the origins of the record amount of Co–C heterolysis in [AdoCbi·1,2-Me₂Im]⁺.

[AdoCbi·bulky base]⁺ Co–C Thermolysis Kinetic Studies. Kinetic studies of the thermolysis of AdoCbi⁺ in the presence of 0.3 M base were accomplished by UV–visible spectroscopy exactly analogous to our recent paper^{5a} (see Figure 2; see also Figures S11, S13, S15, S17, and S19, Supporting Information). The spectra were analyzed by a ln[A_∞/(A_∞ – A_t)] vs time plot at 474 nm [where both

(41) Rappé, A. K.; Casewit, C. J. *Molecular Mechanics across Chemistry*; University Science Books: Sausalito, CA, 1997; pp 22–23.

(42) Lenhart, P. G. *Proc. R. Soc. London, Ser. A* **1968**, *303*, 45.

base-on and base-off Co^{II}Cbi⁺ absorb] to obtain k_{obs} (see Figure 3; see also Figures S12, S14, S16, S18, and S20, Supporting Information). Because the exact percentage of base-on vs base off Co^{II}Cbi⁺ is not known, the data were also analyzed at the isosbestic points obtained from titrating authentic Co^{II}Cbi⁺ with base, resulting in an accurate measurement of the rate of formation of the total amount of Co^{II} (i.e., Co^{II}Cbi⁺ plus [Co^{II}Cbi·bulky base]⁺). All rate constants obtained at both $\lambda = 474$ nm and the isosbestic points proved to be equivalent within experimental error. (For example, for 2,6-Me₂py coordinating to Co^{II}Cbi⁺, an isosbestic point was obtained at 495 nm. Use of the 495 nm data for a first-order kinetic analysis yielded $k_{\text{obs}} = 1.04(6) \times 10^{-5} \text{ s}^{-1}$, which is within experimental error of the value obtained at 474 nm, $k_{\text{obs}} = 1.11(6) \times 10^{-5} \text{ s}^{-1}$.) The results are given in Table 2.

A control was done at the beginning of these kinetic studies to verify that the rate constants measured previously for N-MeIm and py were repeatable: N-MeIm $k_{\text{obs}} = 2.2(6) \times 10^{-5} \text{ s}^{-1}$ (compared with $3.4(6) \times 10^{-5} \text{ s}^{-1}$ previously^{5a}); py $k_{\text{obs}} = 4.8(2) \times 10^{-6} \text{ s}^{-1}$ (compared with $4.6(9) \times 10^{-6} \text{ s}^{-1}$ previously^{4a}). In addition, a series of reactions with variable amounts of 1,2-Me₂Im and 2,6-Me₂py (concentrations ranging from 0.3 to 2.0 M) were completed, and the k_{obs} measured. These results are given in Figure 4 and Figure S25, Supporting Information.

Co^{II}Cobinamide Plus Base Binding Studies. K_{assoc} experiments analogous to those done above for AdoCbi⁺ were carried out in a solution of $1 \times 10^{-4} \text{ M}$ Co^{II}Cbi⁺ and with the same bases and concentrations as used with AdoCbi⁺. The Co^{II}Cbi⁺ was prepared by photolyzing a $1 \times 10^{-4} \text{ M}$ solution of adenosylcobinamide using a sun lamp (equipped with a GE RSM bulb, 275 W, 110–125 V) placed ~30 cm from the reaction flask, in ethylene glycol for 72 h (25 ± 2 °C). However, because Co^{II}Cbi⁺ is air sensitive, all titrations were completed using Schlenk cuvettes with degassed solutions of base under argon. The resulting spectra (see Figure 5, and Figures S7–S10, Supporting Information) were analyzed by our previously established^{4a,5a} methods for determining K_{assoc} via eq 6. This analysis did not yield a linear plot, nor, therefore, a value for $1/K_{\text{assoc}}$. As a control, a Schlenk cuvette^{15,19} containing a solution of Co^{II}Cbi⁺ alone was allowed to stand for 90 min (the time required for a typical titration experiment) to determine whether trace oxygen was a problem; however, no change (<1%) in the absorbance at 468 and 474 nm was seen in the spectra taken during the 90 min of this control experiment, which indicates that trace O₂ is not the reason for the observed lack of isosbestic points. The formation of both α and β isomers of [Co^{II}·base]⁺ is the most likely explanation for the lack of isosbestic points (see the Discussion in the main text).

$$\text{Abs} = \frac{-(\text{Abs} - \text{Abs}_0) \left(\frac{1}{K_{\text{assoc}}} \right) + \text{Abs}_\infty}{[\text{base}_0]} \quad (6)$$

Imidazole and Imidazolate K_{assoc} Product, and Kinetic Studies. A solution of $1 \times 10^{-4} \text{ M}$ AdoCbi⁺ was titrated with a 5.0 M solution of imidazole to determine the K_{assoc} as done above (Figure S6, Supporting Information). The value of K_{assoc} was determined to be 2.9–(3) M⁻¹, a factor 6-fold greater than that of N-MeIm. A solution of $1 \times 10^{-4} \text{ M}$ AdoCbi⁺, 0.3 M N-HIm, and $2 \times 10^{-2} \text{ M}$ TEMPO was thermolyzed at 110.0(2) °C for 23 h (Figure S21, Supporting Information). The k_{obs} was determined using an $\ln[A_\infty/A_\infty - A_t]$ vs time plot, yielding $k_{\text{obs}} = 3.4(6) \times 10^{-5} \text{ s}^{-1}$ (Figure S22, Supporting Information).

A solution of $1 \times 10^{-4} \text{ M}$ AdoCbi⁺, 0.3 M N-HIm, and 0.85 M TEMPO was thermolyzed at 110.0(2) °C for 23 h, and analyzed by HPLC. No heterolysis products could be detected initially, probably because of deprotonation of the expected heterolysis product adenine by the excess imidazole in solution. Glacial acetic acid (8 μL , for a final concentration of 0.3 M) was added to the solution, and the solution heated again for 23 h at 110.0 °C. HPLC analysis of the resulting solution gave 33% adenine, 9% adenine byproduct, and 48% Ado-TEMPO, yielding the same results within experimental error (for both kinetic and product studies) as for AdoCbi⁺ plus N-MeIm.^{5a}

A solution of $1 \times 10^{-4} \text{ M}$ AdoCbi⁺, 0.3 M sodium imidazolate, and $2 \times 10^{-2} \text{ M}$ TEMPO was allowed to stand at 25 °C for 19 h. During this period, the spectrum of AdoCbi⁺ changed cleanly to that of a new corrin product with λ_{max} values at 366, 520, and 560 nm⁴³ while maintaining isosbestic points at 380 and 495 nm (Figure S23, Supporting Information). The resulting final spectrum is unusual, giving rise to a brilliant pink product, believed to be the bis-imidazolate species, [Co^{III}Cbi²⁺·(Im⁻)₂], although a bridged [(Im⁻)Co^{III}Cbi²⁺·Im⁻·Co^{III}Cbi²⁺(Im⁻)⁺] is also possible. An observed rate of $k_{\text{obs}} = 7.37(6) \times 10^{-5} \text{ s}^{-1}$ was obtained through an $\ln[A_\infty/A_\infty - A_t]$ vs time plot, following the growth of the 366 nm peak (Figure S24, Supporting Information). After 19 h, the solution was exposed to air and another visible spectrum taken; no change was observed (i.e., the cobalt product is not air sensitive). HPLC analysis of the solution yielded 105(5)% adenine and no ($\leq 2\%$) detectable homolysis products.

As a control, 4-methylimidazolate was also used to test the effect of a sterically hindered imidazolate. This reaction was set up, run, and analyzed exactly the same as the imidazolate reaction. The results gave $k_{\text{obs}} = 2.3(1) \times 10^{-5} \text{ s}^{-1}$ and complete heterolysis [100(5)% adenine, with no detectable adenine byproduct].

Acknowledgment. Support provided by NIH Grant DK26214 is gratefully acknowledged. We thank Prof. Anthony K. Rappé for helpful discussions of σ vs π effects and assistance in the modeling experiments, as well as the referees whose thoughtful, detailed comments helped improve the final manuscript.

Supporting Information Available: Further discussion of AdoCbi⁺ plus axial-base molecular modeling studies; spectra of attempted AdoCbi⁺ titrations with sterically hindered bases (Figures S1–S6); spectra of Co^{II}Cbi⁺ titrations with sterically hindered bases (Figures S7–S10); spectra and kinetic analyses of the thermolysis of AdoCbi⁺ with sterically hindered bases, including 3-Mepy and 2,5-Me₂py (Figures S11–S25); attempted correlations of molecular modeling and pK_a data with the homolysis and heterolysis rate constants and product ratios (Figures S26–S29); key kinetic derivations; data analysis for 1,2-Me₂Im, 2-Mepy, and 2,6-Me₂py; further discussions of two of the alternative hypotheses for enhanced heterolysis induced by 1,2-Me₂Im; plus a discussion on “A Speculative, but Unifying, Hypothesis for one Unappreciated Role of the Axial-Base.” This material is available free of charge via the Internet at <http://pubs.acs.org>.

IC980608X

- (43) (a) These maxima (366, 520, and 560 nm) are consistent with prior imidazole–cobinamide complexes: Pratt²⁶ reports a λ_{max} value of 357 for a bisimidazolecobinamide species, and a λ_{max} value of 363 nm for an aquoimidazolecobinamide species. In addition, Marzilli^{43b} reports a λ_{max} value of 538 nm for methylimidazolecobinamide. (b) Puckett, J. M., Jr.; Mitchell, M. B.; Hirota, S.; Marzilli, L. G. *Inorg. Chem.* **1996**, *35*, 4656.